SPATIALLY AVERAGED OPEN-CHANNEL FLOW OVER ROUGH BED

By Vladimir Nikora,[1] Derek Goring,[2] Ian McEwan,[3] and George Griffiths[4]

ABSTRACT: In this paper it is suggested that the double-averaged (in temporal and in spatial domains) momentum equations should be used as a natural basis for the hydraulics of rough-bed open-channel flows, especially with small relative submergence. The relationships for the vertical distribution of the total stress for the simplest case of 2D, steady, uniform, spatially averaged flow over a rough bed with flat free surface are derived. These relationships explicitly include the form-induced stresses and form drag as components of the total stress. Using this approach, we define three types of rough-bed flows: (1) Flow with high relative submergence; (2) flow with small relative submergence; and (3) flow over a partially inundated rough bed. The relationships for the double-averaged velocity distribution and hydraulic resistance for all three flow types are derived and compared with measurements where possible. The double-averaged turbulent and form-induced intensities and stresses for the case of regular spherical-segment-type roughness show the dominant role of the double-averaged turbulence stresses and form drag in momentum transfer in the near-bed region.

INTRODUCTION

The turbulence properties of open-channel flows with hydraulically smooth beds have been significantly clarified in the last 20–30 years (Nezu and Nakagawa 1993). Progress was also achieved in understanding the turbulence structure in flows with hydraulically rough beds and high relative submergence [e.g., Grinvald and Nikora (1988), Kironoto and Graf (1994), Song and Graf (1994), Lopez and Garcia (1996), Dittrich and Koll (1997), Nikora and Smart (1997), and Graf and Altinakar (1998)]. At large ratios of flow depth-to-roughness scale the flow structure for most of the depth reveals properties similar to those for flows over smooth boundaries, at least at distances from the bed sufficiently greater than the roughness height. For such flows the logarithmic velocity profile was shown to be valid for the inner flow region, away from the rough bed and water surface. However, the near-bed flow structure in deep flows over irregular rough beds as well as the flow structure of shallow flows with small relative submergence (e.g., gravel-bed rivers, where roughness elements may protrude the flow up to the surface) is still unclear in many respects [e.g., Lopez and Garcia (1996), and Dittrich and Koll (1997)].

Most attempts to clarify the flow structure in the near-bed region of such flows have been based on the Reynolds equations, i.e., time-averaged Navier-Stokes equations, which have served for both modeling and experimental data interpretation. However, the time (or ensemble) averaged flow structure is highly 3D and spatially heterogeneous near irregular rough beds, which makes the time-averaged momentum equations inconvenient and impracticable, e.g., 2D approximations based on the Reynolds equations as well as similarity considerations for time-averaged variables are not possible for the near-bed region. Also, most applications deal with spatially averaged roughness parameters that cannot be linked explicitly with local flow properties provided by the Reynolds equations. Nevertheless, these conceptual contradictions have been essentially ignored in most studies. For instance, in some studies the 2D Reynolds equations were artificially modified by introducing the form drag as an extra body force term and then used to describe the 3D near-bed flow structure. In such studies, mean velocities and turbulence characteristics were implicitly considered as somewhat averaged in the space domain, though the averaging operation was not defined explicitly and all considerations were based on the time-averaged momentum equations. Such an intuitive approach introduces uncertainties in the interpretation of the modeling results. A similar argument applies for interpretation of turbulence measurements taken near rough surfaces.

To avoid this problem conceptually the time (or ensemble) averaging of Navier-Stokes equations should be supplemented by spatial area (or volume) averaging in the plane parallel to the averaged bed. As a result, new continuity and momentum conservation equations may be obtained which are averaged in both time and space domains. They relate to the time-averaged Reynolds equations as the Reynolds equations relate to the Navier-Stokes equations for instantaneous flow variables. Velocities and pressure as well as their moments in these double-averaged equations represent spatially averaged flow parameters which now may be related to the roughness parameters obtained by averaging in the same spatial domain. Another important feature in these new equations is that they include drag terms and form-induced momentum fluxes due to heterogeneity of the time-averaged flow explicitly. These new terms appear naturally as a result of spatial averaging, but not as additional ad hoc terms. Within this approach, similarity hypotheses and 2D assumptions may be developed for double-averaged variables and applied even for the flow region below roughness crests (this is impossible using the conventional Reynolds equations and the time-averaged flow parameters).

In hydraulics the idea of spatial flow averaging was first introduced by Smith and McLean (1977), who considered velocity profiles averaged along lines of constant distance from a wavy bed. The development of a new methodology based on spatially averaged equations was initiated by Wilson and Shaw (1977) for describing atmospheric flows within vegetation canopies. Further contributions have been also made by atmospheric physicists (Raupach and Shaw 1982; Finnigan 1985; Raupach et al. 1991) who provided the mathematical basis for a new set of equations. Recently, Gimenez-Curto and Corniero Lera (1996) successfully applied a similar approach to describe oscillating turbulent flows over very rough surfaces.

The aim of this paper is to consider the potential of this approach for open-channel flows, e.g., gravel-bed canals and rivers, with irregular rough beds. First, we introduce the spatially averaged momentum equations, and using them, subdivide the flow into specific regions. Second, we redefine no-

[1]Sci., Nat. Inst. of Water and Atmospheric Res., P.O. Box 8602, Christchurch, New Zealand.
[2]Sci., Nat. Inst. of Water and Atmospheric Res., P.O. Box 8602, Christchurch, New Zealand.
[3]Sr. Lect., Dept. of Engrg., Univ. of Aberdeen AB24 3UE, U.K.
[4]Sci., Environment Canterbury, P.O. Box 345, Christchurch, New Zealand.

Note. Discussion open until July 1, 2001. To extend the closing date one month, a written request must be filed with the ASCE Manager of Journals. The manuscript for this paper was submitted for review and possible publication on June 7, 1999. This paper is part of the ***Journal of Hydraulic Engineering***, Vol. 127, No. 2, February, 2001. ©ASCE, ISSN 0733-9429/01/0002-0123–0133/$8.00 + $.50 per page. Paper No. 21130.

J. Hydraul. Eng. 2001.127:123-133.

tions of the shear stress distribution and bed shear stress for the case of spatially averaged variables. Finally, we consider potential applications of this approach for such problems as flow resistance and the vertical distribution of flow properties (mean velocity, turbulent, and form-induced intensities and stresses). All our considerations below are for the fixed bed flows although they can be also extended for the mobile-bed flows.

SPATIALLY AVERAGED EQUATIONS

To obtain spatially averaged equations for the near-surface region of the atmospheric boundary layer Wilson and Shaw (1977) and Raupach and Shaw (1982) considered area averaging over a horizontal plane intersecting the vegetation canopy. Later, Finnigan (1985) generalized the area average to a volume average over any volume within the canopy and derived volume-averaged equations. Both approaches are equivalent when the averaging volume is an extensive, infinitesimally thin horizontal slab.

The averaging procedure (for area averaging at level z) is defined as

$$\langle V\rangle(x, y, z, t) = \frac{1}{A_f}\int_{A_f}\int V(x', y,' z, t)\, dx'\, dy' \tag{1}$$

where V = flow variable defined in the fluid but not at points occupied by the roughness elements; angle brackets denote spatial (area) averaging; and A_f = area occupied by fluid within a fixed region on the x,y-plane at level z with the total area A_0. In our considerations we use the right-handed coordinate system (Fig. 1)—x-axis is oriented along the main flow parallel to the averaged bed (u = velocity component), y-axis is oriented to the left bank (v = velocity component), and z-axis is pointing toward the water surface (w = velocity component)—with an arbitrary origin. Below roughness crests the averaging region is multiply connected, since it is intersected by roughness elements. The square root of the area A_0 may be interpreted as a scale of a spatial rectangular window smoothing irregularities with a linear scale $<A_0^{0.5}$. More precisely, two linear scales should be considered, longitudinal L_0 and transverse W_0, $A_0 = L_0W_0$. A convenient choice for scales L_0 and W_0 are longitudinal and transverse correlation lengths of rough bed elevations.

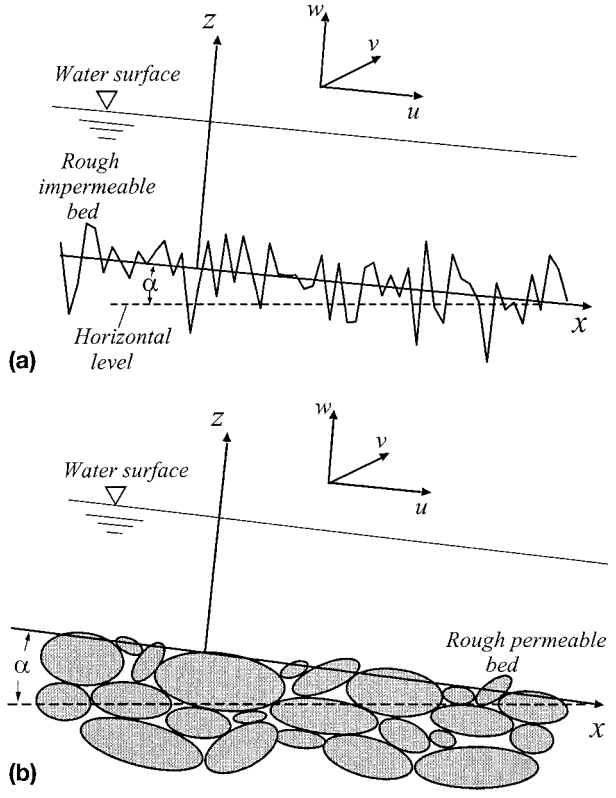

FIG. 1. Sketch for Coordinate Axes: (a) Impermeable Bed; (b) Permeable Bed

In their considerations, Wilson and Shaw (1977), Raupach and Shaw (1982), and Finnigan (1985) assumed that the vegetation canopy is homogeneous. This means that the averaging area A_f does not depend on the coordinates. However, this assumption, being reasonable for vegetation canopies, is not valid when one considers rough surfaces like gravel beds. For such rough surfaces the ratio A_f/A_0 is not constant and usually decreases from roughness crests downward. A variable A_f was incorporated by Gimenez-Curto and Corniero Lera (1996) in their derivation of spatially averaged continuity and momentum conservation equations. When the ratio A_f/A_0 = const their equations reduce to those derived by Raupach and Shaw (1982) and Finnigan (1985). The averaging procedure for the flow region over crests of rough elements does not present any difficulties and simply follows the Reynolds procedure (Monin and Yaglom 1971). The operation of averaging for the flow region below roughness crests is not trivial because operator (1) does not commute with spatial differentiation. Detailed mathematical analysis as well as derivation of the spatially averaged momentum equations are presented by Raupach and Shaw (1982), Finnigan (1985), and Gimenez-Curto and Corniero Lera (1996). In this paper we prefer to use Gimenez-Curto and Corniero Lera's (1996) equations (in a slightly modified form) as more suitable for the purposes of our study.

Applying (1) to the conventional Reynolds equations, i.e.,

$$\frac{\partial \overline{u}_i}{\partial t} + \overline{u}_i\frac{\partial \overline{u}_j}{\partial x_i} = g_i - \frac{1}{\rho}\frac{\partial \overline{p}}{\partial x_i} - \frac{\partial \overline{u_i'u_j'}}{\partial x_j} + \nu\frac{\partial^2 \overline{u}_i}{\partial x_j^2} \tag{2}$$

$$\frac{\partial \overline{u}_i}{\partial x_i} = 0 \tag{3}$$

one can obtain the double-averaged (in time and then in the x,y-plane) momentum and mass conservation equations as

Flow region above the crests of roughness elements $z > z_c$:

$$\frac{\partial \langle\overline{u}_i\rangle}{\partial t} + \langle\overline{u}_i\rangle\frac{\partial \langle\overline{u}_j\rangle}{\partial x_i} = g_i - \frac{1}{\rho}\frac{\partial \langle\overline{p}\rangle}{\partial x_i} - \frac{\partial \langle\overline{u_i'u_j'}\rangle}{\partial x_j} - \frac{\partial \langle\tilde{u}_i\tilde{u}_j\rangle}{\partial x_j} + \nu\frac{\partial^2 \langle\overline{u}_i\rangle}{\partial x_j^2} \tag{4}$$

$$\frac{\partial \langle\overline{u}_i\rangle}{\partial x_i} = 0 \tag{5}$$

Flow region below the crests of roughness elements $z < z_c$:

$$\frac{\partial \langle\overline{u}_i\rangle}{\partial t} + \langle\overline{u}_i\rangle\frac{\partial \langle\overline{u}_j\rangle}{\partial x_i} = g_i - \frac{1}{\rho}\frac{\partial \langle\overline{p}\rangle}{\partial x_i} - \frac{1}{A}\frac{\partial A\langle\overline{u_i'u_j'}\rangle}{\partial x_j} - \frac{1}{A}\frac{\partial A\langle\tilde{u}_i\tilde{u}_j\rangle}{\partial x_j} + \nu\frac{\partial^2 \langle\overline{u}_i\rangle}{\partial x_j^2} + \nu\left\langle\frac{\partial^2 \tilde{u}_i}{\partial x_j^2}\right\rangle - \frac{1}{\rho}\left\langle\frac{\partial \tilde{p}}{\partial x_i}\right\rangle \tag{6}$$

$$\frac{\partial A\langle\overline{u}_i\rangle}{\partial x_i} = 0 \tag{7}$$

where z_c = elevation of the highest roughness crests. In the above equations the straight overbar and angle brackets denote the time and spatial average of flow variables, respectively; the wavy overbar denotes the disturbance in the flow variables, i.e., the difference between time averaged ($\overline{V}$) and double-averaged ($\langle\overline{V}\rangle$) values ($\tilde{V} = \overline{V} - \langle\overline{V}\rangle$), similar to the Reynolds decomposition ($V' = V - \overline{V}$); $g_i = i$th component of the gravity acceleration; ρ = fluid density; ν = kinematic viscosity; and A = ratio of the area A_f occupied by fluid to the total area A_0 of the averaging region. Tensor notation is used for velocity subscripts. Eqs. (4) and (6) describe relations between spatially

J. Hydraul. Eng. 2001.127:123-133.

averaged flow properties and contain some additional terms in comparison with (2). These terms are form-induced stresses, form drag, and viscous drag on the bed. The form-induced stresses $\langle\tilde{u}_i\tilde{u}_j\rangle$ appear as a result of spatial averaging like turbulent stresses $\overline{u_i'u_j'}$ appear in the Reynolds equations as a result of time averaging of the Navier-Stokes equations, i.e., $\langle\tilde{u}_i\tilde{u}_j\rangle$ are due to spatial disturbances in time-averaged flow. To identify $\langle\tilde{u}_i\tilde{u}_j\rangle$ Wilson and Shaw (1977) used the term ''dispersive stresses'' while Gimenez-Curto and Corniero Lera (1996) prefer the term ''form-induced stresses.'' In this paper we will use the latter term. The form drag $(1/\rho)\langle\partial\tilde{p}/\partial x_i\rangle$ and viscous drag $\nu\langle\partial^2\tilde{u}_i/\partial x_j^2\rangle$ on the bed appear only in equations for the flow region below roughness crests [(6)]. Also, the equations of motion for the flow region below the roughness crests [(6) and (7)], demonstrate dependence on the roughness geometry, i.e., on the parameter A. This parameter is important if the roughness elements change their density and cross sections with coordinates; it disappears if they do not. The only difference between equations (4)–(7) and those derived by Gimenez-Curto and Corniero Lera (1996) is that instead of area A_f we use the normalized parameter $A = A_f/A_0$ which we call a roughness geometry function $A = F(x, y, z)$.

In this paper we consider the simplest case of 2D, steady, uniform, spatially averaged flow over a rough bed with flat free surface. Such a flow possesses the following properties: (1) The time-averaged flow variables do not change in time (i.e., there are no long-term trends in flow properties, and all variations are due to turbulence only); (2) the vertical change in spatially averaged flow properties is significantly stronger than longitudinal and transverse ones; (3) the spatially averaged vertical $\langle\tilde{w}\rangle$, and transverse $\langle\tilde{v}\rangle$, velocities are equal to zero, and there is no correlation between u and v and between v and w; (4) the water surface is flat; (5) the bed roughness [i.e., the field of bed elevations $Z_b(x, y)$] is ''frozen'' and statistically homogeneous in the x,y-plane, i.e., the roughness geometry function A depends only on the vertical coordinate z, i.e., $A = A(z)$. For high Reynolds number 2D flows (4) and (6) reduce to (see sketch in Fig. 1 for symbols)

Flow region above the roughness crests $z > z_c$:

$$gS_b - \frac{\partial\langle\overline{u'w'}\rangle}{\partial z} - \frac{\partial\langle\tilde{u}\tilde{w}\rangle}{\partial z} = 0 \tag{8a}$$

$$g\cos\alpha + \frac{1}{\rho}\frac{\partial\langle\overline{p}\rangle}{\partial z} + \frac{\partial\langle\overline{w'^2}\rangle}{\partial z} + \frac{\partial\langle\tilde{w}^2\rangle}{\partial z} = 0 \tag{8b}$$

Flow region below the roughness crests $z < z_c$:

$$gS_b - \frac{1}{\rho}\left\langle\frac{\partial\tilde{p}}{\partial x}\right\rangle - \frac{1}{A}\frac{\partial A\langle\overline{u'w'}\rangle}{\partial z} - \frac{1}{A}\frac{\partial A\langle\tilde{u}\tilde{w}\rangle}{\partial z} = 0 \tag{9a}$$

$$g\cos\alpha + \frac{1}{\rho}\frac{\partial\langle\overline{p}\rangle}{\partial z} + \frac{1}{\rho}\left\langle\frac{\partial\tilde{p}}{\partial z}\right\rangle + \frac{1}{A}\frac{\partial A\langle\overline{w'^2}\rangle}{\partial z} + \frac{1}{A}\frac{\partial A\langle\tilde{w}^2\rangle}{\partial z} = 0 \tag{9b}$$

Eqs. (8a) and (9a) are for the longitudinal velocity component while (8b) and (9b) are for the vertical one. Equations for the transverse velocity disappear. We also neglect viscous terms in (8a)–(9b) because of the high Reynolds number. The parameter S_b is the slope of the averaged bed, $S_b \approx \sin\alpha$ (Fig. 1), which is equal to the downgradient slope of the water surface. We use (8a)–(9b) in our following considerations. Before proceeding further, we first consider some properties of the roughness geometry function A.

ROUGHNESS GEOMETRY FUNCTION $A(z)$

An important feature of (6), (7), (9a), and (9b) is the dependence on the roughness geometry which is taken into account by the function $A(z)$, $1 \geq A(z) \geq A_{\min} \geq 0$. In the region above roughness crests $A \equiv 1$. When the lower limit $A_{\min} = 0$ we have an impermeable bed [Fig. 2(a)] while for permeable beds $A_{\min} > 0$ [Fig. 2(b)]. For irregular impermeable rough beds [Fig. 2(a)] we can define the function $A(z)$ as the cumulative probability distribution of bed elevations, i.e., the probability for a bed elevation Z_b to be less than a given elevation z. The interpretation of $A(z)$ as $A(z) = P(Z_b < z)$ is valid only if $Z_b(x, y)$ is a single-valued function. It is worth noting that G. Parker (personal communication, 1999) uses a similar approach to describe bed topography in his revision of Hirano's concept of the active layer. In his considerations he used the cumulative distribution $p_s = P(Z_b > z)$, which relates to $A(z)$ as $p_s(z) = 1 - A(z)$. For granular surfaces, single-valued bed topography can be expected if the particle size D is small enough so that any micromotions of the interstitial fluid may be neglected, at least for the purposes of this study. Typical examples from fluvial hydraulics are sand wave surfaces (ripples and dunes) and the rough surfaces of cohesive soils. For such surfaces the particle size D is much smaller than the height Δ of roughness elements created from these particles, i.e., $(D/\Delta) << 1$. At the other extreme, when particles are large, interstitial motions are not negligible, and $(D/\Delta) \approx 1$, we have permeable beds [Fig. 2(b)] whose topography $Z_b(x, y)$ is not single-valued anymore. A typical example is a gravel surface where the roughness elements are presented by particles with a narrow unimodal size distribution, or by assemblages of a few gravel particles. From these considerations, the roughness geometry function $A(z)$ is a statistical measure of both the random geometry of the bed surface and the permeability. In the case of permeable beds, at z below the surface particles, the function $A(z)$ is analogous to the porosity coefficient of the granular material.

Fig. 3 shows examples of $A(z)$ for water-worked gravel beds (New Zealand rivers) and unworked gravel beds created manually in two flumes (Nikora et al. 1998a). Detailed analysis of measured gravel-bed profiles using the random field approach is presented in Nikora et al. (1998a). Here we use results of that study to show that empirical functions $A(z)$ for both natural rivers and flumes behave similarly and are fairly close to

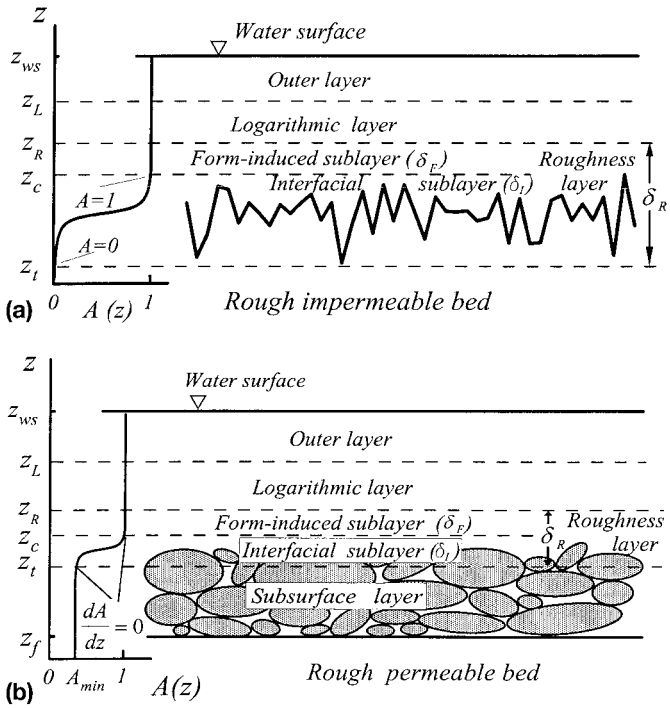

FIG. 2. Flow Subdivision into Specific Regions: (a) Impermeable Bed; (b) Permeable Bed

J. Hydraul. Eng. 2001.127:123-133.

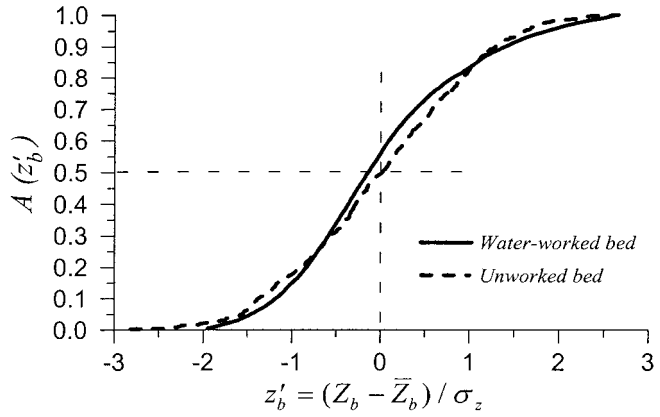

FIG. 3. Roughness Geometry Function $A(z)$ for Water-Worked and Unworked Gravel Beds: Averaged Functions $A(z)$ Are Presented, Z_b Is Bed Elevation, $\overline{Z}_b$ Is Average Bed Elevation, and σ_z Is Standard Deviation of Bed Elevations (Data from Nikora et al. 1998a)

the cumulative probability function for the normal distribution. Unfortunately, the applied measurement procedure did not permit us to get information about $A(z)$ at z lower than those for particles lying on the bed surface. Therefore, the empirical functions $A(z)$ in Fig. 3 characterize only an interfacial sublayer [Fig. 2(b)] between the flow and the gravel bed, and present no information about the gravel-bed porosity. In the subsurface gravel layer the function $A(z)$ changes insignificantly and does not exceed the range 0.2–0.3 (Linsley et al. 1975). In some cases, when the interstitial space between large particles (e.g., gravel) is filled with much smaller particles (e.g., sand), we can assume $A_{\min} \approx 0$ and the bed may be fairly considered as ''impermeable,'' with single-valued topography.

SUBDIVISION OF FLOW INTO SPECIFIC LAYERS

Eqs. (8*a*)–(9*b*) are written for two flow regions, above and below roughness crests. The main reason for such a subdivision was the appearance of the additional terms and variables in the equations for the flow region below z_c. However, a further subdivision is also possible when one considers the significance of some terms in (8*a*)–(9*b*). For the purposes of this paper we suggest the following flow subdivision (Fig. 2), assuming $H >> \Delta$, where H is the maximum depth equal to the distance between water surface and troughs of roughness elements, i.e., $H = z_{ws} - z_t$ (Fig. 2).

1. Outer layer: In this region the viscous effects and form-induced fluxes are negligible and the spatially averaged equations are identical to the time-averaged equations. Characteristic scales for this layer are the shear velocity u_*, the maximum flow velocity $U_{\max}$, the distance from the bed, and the flow depth H, where $u_* = (\tau_0/\rho)^{0.5}$ and τ_0 is the bed shear stress. This layer includes the near-surface and intermediate regions, in the sense of Nezu and Nakagawa (1993), and is similar to the outer layer for open-channel flows over hydraulically smooth beds. The velocity distribution in this layer may be described by the velocity defect law (Nezu and Nakagawa 1993).

2. Logarithmic layer: In this flow region the viscous effects and form-induced fluxes are negligible and the spatially averaged equations are identical to the time-averaged equations, as for the outer layer. However, the characteristic scales for the logarithmic layer are different from those for the outer layer. These scales are the shear velocity u_*, the distance from the bed, and characteristic scales of the bed topography. The appropriate candidates for such scales, for irregular bed roughness, are the standard deviation of bed elevations and longitudinal and transverse correlation lengths (Nikora et al. 1998a). This layer is similar to the logarithmic layer for flows with hydraulically smooth beds, and may be identified as the equilibrium layer in Townsend's (1998) sense. Note that for rough-bed flows this layer has been defined in terms of time-averaged velocities (Raupach et al. 1991), i.e., the distribution of $\overline{u}$ in this layer follows the logarithmic formula. A crucial condition for the existence of this layer is $H >> \Delta$. The logarithmic layer occupies the flow region $(2 - 5)\Delta < (z - z_t) < 0.2H$ (Raupach et al. 1991; Nezu and Nakagawa 1993).

3. Form-induced sublayer: The flow in this region is influenced by individual roughness elements and all the terms in (8*a*) and (8*b*) may be important. The form-induced sublayer occupies the region just above the roughness crests, subject to (8*a*) and (8*b*). The name ''form-induced'' reflects the appearance of a new feature in this sublayer, in comparison with the logarithmic layer, namely the form-induced stresses which are due to flow separation from the roughness elements (Gimenez-Curto and Corniero Lera 1996). According to Raupach et al. (1991) the roughness elements may influence the local flow structure within $0 < z - z_c < (1 - 4)\Delta$, i.e., the thickness of the form-induced sublayer, $\delta_F = z_R - z_c$ (Fig. 2), may be up to $(1 - 4)\Delta$.

4. Interfacial sublayer: This sublayer is also influenced by individual roughness elements and occupies the flow region between roughness crests and troughs, i.e., where the roughness geometry function $A(z)$ changes from 1 to 0 for impermeable beds, or from 1 to $A_{\min}$ for permeable beds (Fig. 2), subject to (9*a*) and (9*b*). A new important feature in this sublayer is that associated with form drag. The thickness of the interfacial sublayer is defined as $\delta_I = z_c - z_t$ (Fig. 2).

The form-induced and interfacial sublayers together may be identified as the roughness layer. We prefer the term ''roughness layer'' instead of the ''roughness sublayer'' from Raupach et al. (1991) as we subdivide this layer into two sublayers, the form-induced and interfacial sublayers. The main characteristic scales of the roughness layer are the shear velocity u_* and characteristic lengths of the bed topography. Similar to boundary layers with hydraulically smooth beds, we can identify the flow region occupied by the logarithmic and roughness layers as the wall or inner layer. The same analogy suggests that the role of the roughness layer for hydraulically rough beds is similar to that of the viscous and buffer sublayers for smooth beds (Nikitin 1963, 1980; Raupach et al. 1991). The interfacial sublayer can be interpreted in a manner similar to the viscous sublayer while the form-induced sublayer is analogous to the buffer sublayer.

The above four regions cover the whole open-channel flow over an impermeable rough bed. When the bed is permeable an additional, subsurface, layer should be also considered.

5. Subsurface layer: The flow in this layer occupies pores between granular particles and is driven by the gravity force and momentum fluxes from the above layers. The upper boundary of the subsurface layer (lower boundary of the interfacial sublayer) may be identified at z where $dA/dz \approx 0$ [Fig. 2(b)]. The characteristic scales of the subsurface layer are the shear velocity u_* and pore characteristic lengths.

The following flow types, depending on the relative smoothness (flow depth H/roughness height Δ), may be deduced from the above subdivision: (1) Flow with high relative submergence ($H >> \Delta$), which contains all the above sublayers; (2) flow with small relative submergence [$(2 - 5)\Delta > H \geq \Delta$], with the form-induced sublayer as the upper flow region; and (3) flow over partially inundated rough bed ($H < \Delta$), with the interfacial sublayer as the upper flow region. We use the above flow subdivision and flow types in our following considerations.

J. Hydraul. Eng. 2001.127:123-133.

TOTAL SHEAR STRESS AND PRESSURE

The vertical distribution of spatially averaged pressure in the flow region above the roughness crests can be determined by integrating (8*b*) from z to the water surface. This yields

Outer and logarithmic layers:

$$\langle \overline{p} \rangle(z) = \overline{p}(z) = \rho g \cos \alpha [z_{ws} - z] + \rho [\langle \overline{w'^2} \rangle (z_{ws}) - \langle \overline{w'^2} \rangle (z)]$$
$$\approx \rho g \cos \alpha [z_{ws} - z] - \rho \langle \overline{w'^2} \rangle (z) \approx \rho g \cos \alpha [z_{ws} - z]$$
$$- \rho \overline{w'^2}(z) \tag{10}$$

Form-induced sublayer:

$$\langle \overline{p} \rangle(z) = \rho g \cos \alpha [z_{ws} - z] + \rho [\langle \overline{w'^2} \rangle (z_{ws}) - \langle \overline{w'^2} \rangle (z)]$$
$$+ \rho [\langle \tilde{w}^2 \rangle (z_{ws}) - \langle \tilde{w}^2 \rangle (z)] \approx \rho g \cos \alpha [z_{ws} - z]$$
$$- \rho \langle \overline{w'^2} \rangle (z) + \langle \tilde{w}^2 \rangle (z)] \tag{11}$$

where z_{ws} = elevation of the water surface (Fig. 2). (Please note that parentheses are used for arguments.) Eq. (10) is similar to that for the time-averaged flow. In (11) an additional term, $\langle \tilde{w}^2 \rangle$, appears that increases the deviation from the hydrostatic distribution, compared to the logarithmic layer. This term is negligible in the region far from the bed surface but can be important in the region close to the roughness crests, i.e., in the form-induced sublayer. The analytical integration of (9*b*) for the region below the roughness crests (i.e., for the interfacial sublayer and subsurface layer) is not possible. In general, (9*b*) suggests that the pressure distribution in this flow region should strongly depend on the bed surface geometry and particle composition, and may significantly deviate from the hydrostatic distribution. Experimental and numerical investigations of this problem would be useful to clarify the potential pressure contribution to the initiation of bed particle motion.

In similar fashion, integration of (8*a*) and (9*a*) produces the following relationships for the total stress distribution:

Outer and logarithmic layers

$$\frac{\tau(z)}{\rho} = g S_b [z_{ws} - z] = -\langle \overline{u'w'} \rangle (z) = -\overline{u'w'}(z) \tag{12}$$

Form-induced sublayer

$$\frac{\tau(z)}{\rho} = g S_b [z_{ws} - z] = [-\langle \overline{u'w'} \rangle (z) - \langle \tilde{u}\tilde{w} \rangle (z)] \tag{13}$$

Interfacial sublayer

$$\frac{\tau(z)}{\rho} = g S_b \left\{ z_{ws} - z_c + \int_z^{z_c} A(z)\, dz \right\} = [-A \langle \overline{u'w'} \rangle (z) - A \langle \tilde{u}\tilde{w} \rangle (z)]$$
$$+ \int_z^{z_c} \frac{A(z)}{\rho} \left\langle \frac{\partial \tilde{p}}{\partial x} \right\rangle dz \tag{14}$$

Subsurface layer

$$\frac{\tau z}{\rho} = g S_b \left\{ z_{ws} - z_c + \int_{z_t}^{z_c} A(z)\, dz + A_{\min} [z_t - z] \right\}$$
$$= A_{\min} [-\langle \overline{u'w'} \rangle (z) - \langle \tilde{u}\tilde{w} \rangle (z)] + \int_{z_t}^{z_c} \frac{A(z)}{\rho} \left\langle \frac{\partial \tilde{p}}{\partial z} \right\rangle dz$$
$$+ \frac{A_{\min}}{\rho} \int_z^{z_t} \left\langle \frac{\partial \tilde{p}}{\partial x} \right\rangle dz \tag{15}$$

where z_t = lower boundary of the interfacial sublayer (Fig. 2). From (12) and (13) it follows that for the region above the roughness crests the gravity force $g S_b [z_{ws} - z]$ is balanced by the turbulent shear stress (the outer and logarithmic layers), and the form-induced shear stress (form-induced sublayer). To balance the gravity force below the roughness crests (the interfacial sublayer and subsurface layer) the turbulent and form-induced stresses are supplemented with additional stresses due to the form drag [(14) and (15)].

For impermeable rough beds (15) is not relevant and the bed shear stress τ_0 can be defined from (14) as

$$\frac{\tau_0}{\rho} = \frac{\tau(z_t)}{\rho} = g S_b [z_{ws} - z_c + h_w] = \int_{z_t}^{z_c} \frac{A(z)}{\rho} \left\langle \frac{\partial \tilde{p}}{\partial x} \right\rangle dz \tag{16}$$

where $h_w = \int_{z_t}^{z_c} A(z)\, dz = (1/A_0) \int_{z_t}^{z_c} A_f(z)\, dz$ = thickness of water layer with the base area A_0 and volume equivalent to water volume in the interfacial sublayer. The turbulent and form induced stresses disappear in (16); since at $z = z_t$ they are both zero. Similarly, for permeable rough beds [Fig 2(b)] we can obtain from (14) the following:

$$\frac{\tau_0}{\rho} = \frac{\tau(z_t)}{\rho} = g S_b [z_{ws} - z_c + h_w] = [-A \langle \overline{u'w'} \rangle (z_t) - A \langle \tilde{u}\tilde{w} \rangle (z_t)]$$
$$+ \int_{z_t}^{z_c} \frac{A(z)}{\rho} \left\langle \frac{\partial \tilde{p}}{\partial x} \right\rangle dz \tag{17}$$

Eq. (17) differs from that for impermeable beds [(16)] by nonzero turbulent and form-induced fluxes at $z = z_t$. These fluxes reflect momentum exchange between the channel flow and the subsurface flow. Also, comparing (16) and (17) one can see that at the same flow depth and bed geometry the drag term for permeable beds may be different from that for impermeable beds. This means that the actual forces acting on the roughness elements within the interfacial sublayer of the flow over permeable beds may be changed at the expense of turbulent and form-induced fluxes. The shear stress at z_f, i.e., at the impermeable floor supporting particles (e.g., the valley floor bedrock of a gravel-bed stream), can be defined from (15) as

$$\frac{\tau_f}{\rho} = \frac{\tau(z_f)}{\rho} = g S_b \{ z_{ws} - z_c + h_w + A_{\min} [z_t - z_f] \}$$
$$= \int_{z_t}^{z_c} \frac{A(z)}{\rho} \left\langle \frac{\partial \tilde{p}}{\partial z} \right\rangle dz + \frac{A_{\min}}{\rho} \int_{z_f}^{z_t} \left\langle \frac{\partial \tilde{p}}{\partial x} \right\rangle dz \tag{18}$$

VELOCITY DISTRIBUTION AND HYDRAULIC RESISTANCE

At the beginning of our considerations we have accepted the coordinate system with an arbitrary origin. However, in many cases it is useful to deal with a physically based origin since distance from this datum may serve as an inherent characteristic scale, e.g., in some situations the mixing length is proportional to this distance that leads to the semilogarithmic velocity distribution. For flows over smooth impermeable flat beds it is not a problem as the natural choice for such an origin is the surface of the flat bed. However, for rough beds the position of the reference bed (or the zero-plane) has to be defined and a displaced coordinate $Z = (z - d_p)$ instead of z should be considered. The length d_p is known as the displacement length or the zero-plane displacement. For flow over a smooth flat bed we have $\overline{u} = 0$ and $\tau = \tau_0$ at $z = 0$ corresponding to the bed elevation. By analogy, we can define the reference level for impermeable rough-bed flows at z_t where $\langle \overline{u} \rangle = 0$ and $\tau = \tau_0$. Thus, we have $d_p = z_t$ and assume that $A(z_t) = 0$, as in Fig. 2(a). However, in general $A(z_t)$ may be nonzero as well as the position of the reference bed may be higher, i.e., $d_p > z_t$. One also may argue that for rough bed flows the conditions $\overline{u} = 0$ and $\tau = \tau_0$ at $z = 0$ may be reduced to only

J. Hydraul. Eng. 2001.127:123-133.

$\overline{u} = 0$. Analytical or numerical solutions of (8*a*)–(9*b*) are not possible without parameterization of the spatially averaged turbulent stresses, $\rho\langle\overline{u'w'}\rangle$, form-induced stresses, $\rho\langle\tilde{u}\tilde{w}\rangle$, and the form drag, $\rho\langle\partial\tilde{p}/\partial x\rangle$. Specifically designed experiments are required to properly develop such physically based parameterizations. Here we consider this problem at the heuristic level only, i.e., using some reasonable assumptions and scaling considerations.

Flow Type 1 ($H >> \Delta$)

The velocity distribution in the outer layer is similar to that for flows over hydraulically smooth beds (Nezu and Nakagawa 1993; Graf and Altinakar 1998) and is not considered here. Applying reformulation of Izakson's (1937) overlap approach [also described by Millikan (1939)], for spatially averaged velocity $\langle\overline{u}\rangle$, we obtain for the logarithmic layer

$$\frac{\langle\overline{u}\rangle(Z)}{u_*} = \frac{1}{\kappa}\ln\left[\frac{Z}{\delta_R}\right] + \frac{\langle\overline{u}\rangle(\delta_R)}{u_*} \tag{19}$$

where κ = von Kármán constant; $Z = z - z_t$; and $\delta_R = z_R - z_t$ with z_R as a lower bound of the logarithmic layer (Fig. 2). Izakson's (1937) approach was initially developed for the time-averaged velocity $\overline{u}$ and is formally extended here to the spatially averaged velocity $\langle\overline{u}\rangle$. To parameterize velocity distribution in the interfacial sublayer we use an analogy with the viscous sublayer. In this sublayer, the contribution of viscous stresses to the total stress increases toward the bed while that of turbulent stresses decreases. In the interfacial sublayer, the form-induced stresses and the form drag play a role similar to the viscous stresses in the viscous sublayer. Using this analogy we can formally propose for the interfacial sublayer

$$\frac{\tau(Z)}{\rho} = \nu_I\frac{d\langle\overline{u}\rangle}{dZ} \tag{20}$$

where ν_I = generalized viscosity that represents a joint effect of the form-induced stresses and form drag, just as ν represents the molecular viscosity of the fluid in the viscous sublayer. Assuming, as a first approximation, that ν_I does not change with Z, $\tau(Z)/\rho \approx \tau_0/\rho = u_*^2$, and bearing in mind that $\langle\overline{u}\rangle = 0$ at $Z = 0$, we can obtain from (20)

$$\frac{\langle\overline{u}\rangle(Z)}{u_*} = \frac{u_*}{\nu_I}Z = \left\{\frac{\langle\overline{u}\rangle(\delta_I)}{u_*}\right\}\frac{Z}{\delta_I} \tag{21}$$

where $\nu_I = [u_*/\langle\overline{u}\rangle(\delta_I)]u_*\delta_I$; and $\delta_I = z_c - z_t$ (Fig. 2). The role of the form-induced sublayer, with the thickness $\delta_F = z_R - z_c = \delta_R - \delta_I$, is similar to that of the buffer sublayer for flows over hydraulically smooth beds. Here, as a first approximation, we neglect the potential transition effects in the form-induced sublayer and assume that $z_R \approx z_I$, i.e., $\delta_F \to 0$. This leads to $\delta_R \approx \delta_I = \delta$, where δ is the boundary between the logarithmic and linear flow regions when the coordinate $Z = z - z_t$ is used. One can note that this approximation is similar to the two-layer Prandtl's model for smooth-bed flows (Monin and Yaglom 1971), which neglects the transition effects in the buffer sublayer. As a result of the above consideration we arrive at a simplified three-layer model for open-channel flow over a hydraulically rough bed, which includes (1) An outer layer (not considered here), (2) a logarithmic layer, and (3) a linear or interfacial sublayer. The velocity distribution for the latter two can be expressed as

$$\frac{\langle\overline{u}\rangle}{u_*} = \frac{1}{\kappa}\ln\left[\frac{Z}{\delta}\right] + C \quad \text{for} \quad (z_L - z_t) \geq Z \geq \delta \tag{22}$$

$$\frac{\langle\overline{u}\rangle}{u_*} = C\frac{Z}{\delta} \quad \text{for} \quad 0 \leq Z \leq \delta \tag{23}$$

where $C = \langle\overline{u}\rangle(\delta)/u_*$ should depend on the roughness geometry; and z_L = upper boundary of the logarithmic layer (Fig. 2). Note that relationship (22) for the double-averaged velocity $\langle\overline{u}\rangle$ extends the logarithmic layer for $\overline{u}$, as specified in the section ''Subdivision of Flow into Specific Layers,'' up to the roughness crests. The validity of relationship (22) above the roughness sublayer (where $\langle\overline{u}\rangle = \overline{u}$) has been confirmed in many studies (Grinvald and Nikora 1988; Raupach et al. 1991; Nezu and Nakagawa 1993). To test the validity of the assumption $\delta_R \approx \delta_I = \delta$ and relationship (23) one would require measurements of $\langle\overline{u}\rangle$ as $\overline{u}$ cannot be a substitute for $\langle\overline{u}\rangle$ in the form-induced and interfacial sublayers. Unfortunately, direct velocity measurements in the roughness layer are rare, and, moreover, mainly relate to $\overline{u}$. We are aware of only one set of measurements that provides information of $\langle\overline{u}\rangle$. This set was obtained in a small gravel-bed flume by Nikitin (1963), who glued gravel particles, with the size distribution similar to that in natural streams, to the flat flume bed. Nikitin's (1963) technique was based on the analyses of flow photographs and microphotographs and allowed him to obtain time- and spatially averaged velocities within the roughness layer and above it. From Nikitin's (1963) measurements it follows that the $\langle\overline{u}\rangle$-velocity distribution below roughness tops is linear with $C = 5.6$ [he confirmed this value in a later work (Nikitin 1980)]. Similar results were also reported by Dittrich and Koll (1997) who measured velocities below roughness tops using laser Doppler anemometer. The flume bed in their experiments was densely covered by gravel particles with very narrow size distribution. The data of Dittrich and Koll (1997, p. 30) show that the velocity distribution below roughness tops was fairly linear with $C \approx 5.3$. The flume experiments of Shimizu et al. (1990, p. 71) with glass beads on the bed show very similar results, i.e., linearity of the velocity distribution within the interfacial sublayer with $C \approx 5.7$–6.0. Our laboratory data also support the validity of (23) as well as provide some support for $\delta_R \approx \delta_I = \delta$. The measurements, using SonTek's Acoustic Doppler Velocimeters (ADV) (Kraus et al. 1994; Lohrmann et al. 1994; Nikora and Goring 1998), were made in a 12-m-long and 0.75-m-wide flume (Nikora et al. 1998b). The flume bed was covered by 1.2-mm-thick styrene sheets with thin (0.3–0.4 mm) flocked (''velvet'') coating with spherical segments [diameter of a sphere = 63.8 mm, segment height = 21 mm; Fig. 4(a)]. The roughness geometry function $A(Z)$ for this artificial bed is shown in Fig. 4(b). The measurements were made at two flow rates, low (#1) and high (#2) (Table 1). Two identical patterns [Fig. 4(a)] were measured synchronously by two ADV probes with a distance between them of 350 mm. Each pattern included 16 measurement verticals [crosses and diamonds in Fig. 4(a)] for the low flow, and seven verticals [crosses in Fig. 4(a)] for the high flow. At each vertical, 3D velocities were measured at 10–14 points. Although the measured data set has insufficient spatial coverage to obtain very accurate values of $\langle\overline{u}\rangle$, it still can be used for a test of relationships (22) and (23). Fig. 4(c) shows the distributions of time-averaged longitudinal velocities as well as the curves representing relationships (22) and (23) with parameters from Table 1. These solid lines approximate the data quite well, supporting both relationships (22) and (23), and the assumption $\delta_R \approx \delta_I = \delta$. It is remarkable that the distribution of the double-averaged velocity reveals logarithmic behavior even at modest ratios of $H/\Delta = 6.4$–8.7 (as before, $H = z_{ws} - z_t$ and Δ is the height of spherical segments; Table 1). Also, Fig. 4(c) clearly shows that the deviation of time-averaged velocities from the logarithmic curve, i.e., $\tilde{u} = \overline{u} - \langle\overline{u}\rangle$, decreases with increase in distance from the bed, as one would expect from our theoretical considerations. The parameter $C = 7.1$ (Table 1) appeared to be different from $C = 5.3$–6.0 for Nikitin's (1963, 1980) and Dittrich and Koll's

J. Hydraul. Eng. 2001.127:123-133.

(1997) gravel-bed data, and Shimizu et al.'s (1990) glass-bead bed data, which is probably due to differences in the roughness geometry.

Additional estimates for C can be made using the existing log-based formulas for hydraulic resistance for rough-bed flows over homogeneous sand roughness and nonhomogeneous gravel roughness. These formulas allow one to make approximate estimates for δ and C using five assumptions: (1) The thickness of the interfacial sublayer δ_I of homogeneous sand roughness is equal to the sand diameter D, $\delta_R \approx \delta_I = \delta \approx \Delta \approx D$, as was assumed by Nikuradse (Monin and Yaglom 1971); (2) the thickness δ of the interfacial sublayer of water-worked gravel beds is approximately equal to $4\sigma_b \approx 1.5D_{50}$, where σ_b is the standard deviation of bed elevations and D_{50} is the 50th percentile of particle size distribution of the surface material (Nikora et al. 1998a); (3) the resistance of water-worked gravel beds is due to gravel particles, i.e., bed-form effects are negligible; (4) for the flow region above the roughness layer we have $\langle\overline{u}\rangle = \overline{u}$, and therefore, formulas for hydraulic resistance, based on $\overline{u}$, are also valid for $\langle\overline{u}\rangle$; and (5) for flows with $H >> \Delta$ the contribution from the roughness layer to the vertically-mean velocity is negligible as well as the difference between the maximum and mean depths.

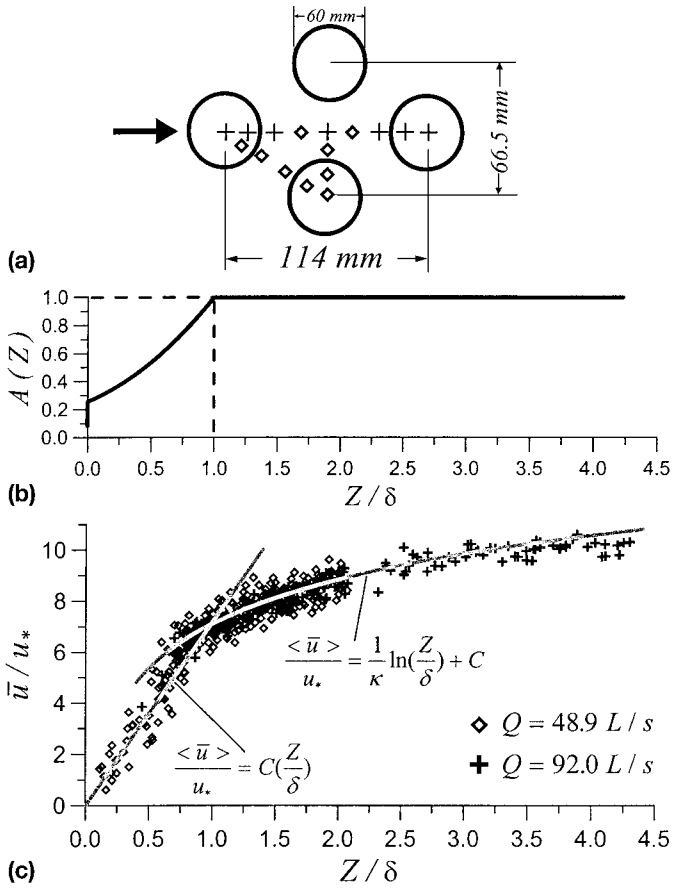

FIG. 4. Position of (a) Measurement Verticals; (b) Roughness Geometry Function; (c) Velocity Distribution for Flow Measurements over Spherical Segment-Type Bed (Table 1)

To define C for the homogeneous sand roughness one can use Nikuradse's formula $U/u_* = 2.5\ \ln[H/D] + 6.0$ (Monin and Yaglom 1971), which gives $C \approx 8.5$ comparable with our $C \approx 7.1$ for spherical segment-type bed (U is the depth-averaged velocity). For the water-worked gravel roughness the parameters δ and C should depend on particle size distribution, particle shape, and spatial arrangements, which are known to be similar for different rivers (Bathurst 1985a; Bray 1985; Nikora et al. 1998a). This similarity suggests that the range of C for natural gravel-bed flows should be fairly narrow. For our estimates we have selected two formulas: (1) $U/u_* = 2.434 \cdot \ln[H/D_{50}] + 2.15$, developed by Griffiths (1981) for New Zealand rivers; and (2) $U/u_* = 2.5 \cdot [H/D_{50}] + 1.46$, developed by Bray (1985) for Canadian rivers. The obtained estimates are $C = 5.6$ (from Griffiths' formula) and $C = 5.0$ (from Bray's formula). The value $C = 5.6$ for the New Zealand data is remarkably close to those that follow from laboratory experiments of Nikitin (1963) and Dittrich and Koll (1997). The latter value, $C = 5.0$, is less reliable as we have used the relationship $4\sigma_b \approx 1.5D_{50}$ derived from the New Zealand data (Nikora et al. 1998a) to obtain C for the Canadian data. Thus, we can accept, as a first approximation, $C \approx 8.5$ for the homogeneous sand roughness and $C \approx 5.3$–5.6 for the natural and artificial gravel beds. The above estimates provide quite encouraging support for our three-layer model. However, we consider it as a first approximation only.

All three layers (outer, logarithmic, and interfacial) in our simplified model have smooth-bed flow counterparts with similar behavior. This suggests that our considerations may be equally valid for both rough- and smooth-bed flows if applied for double-averaged (in spatial and time domains) velocities. Indeed, for smooth-flat-bed flows the double-averaged velocities are equivalent to the time-averaged velocities, while $\delta \approx 11.1[\nu/u_*]$ and $C \approx 11.1$ which follow from the smooth-wall logarithmic law $\overline{u}/u_* = 2.5\ \ln[u_* z/\nu] + 5.1$ (Monin and Yaglom 1971). It should be noted that Nikitin (1963) was the first who suggested such an analogy between smooth-bed and rough-bed flows (his main argument was the linearity in velocity distribution near the rough bed). Unfortunately, all his interpretations were based on the conventional time-averaged Reynolds equations which cannot be used as a basis for scaling or phenomenological considerations for the near-bed region in rough-bed flows.

TABLE 1. Hydraulic Conditions and Parameters of Relationships (22) and (23) for Experiments with Flows over Bed Covered with Spherical Segments of Height $\Delta = 2.1$ cm

Flow rate number (1)	Q (L/s) (2)	S_b (3)	H (cm) (4)	u_{*s}[a] (cm/s) (5)	u_{*b}[b] (cm/s) (6)	Parameters of Relationships (22) and (23)				u_*[d] (cm/s) (11)	$u_*\Delta/\nu$ (12)
						u_{*L}[c] (cm/s) (7)	κ (8)	C (9)	δ (cm) (10)		
1	48.9	0.0032	13.5	6.5	6.6	6.4	0.40	7.1	2.1	6.5	1,365
2	92.0	0.0031	18.2	7.6	7.8	7.7	0.40	7.1	2.1	7.7	1,617

[a] $u_{*s} = \sqrt{\tau_0/\rho}$ is shear velocity obtained by extrapolation of near-bed values of $-\langle\overline{u'w'}\rangle$ to mean bed level $\overline{Z}_b = Z_c - \int_{z_t}^{z_c} A(z)\,dz$, according to Eqs. (12)–(14), (16), and Fig. 7, assuming that form-induced stresses are negligible (Fig. 8 confirms that in form-induced sublayer $\langle u'w'\rangle >> \langle\tilde{u}\tilde{w}\rangle$), $Z_c = z_c - z_t$ with z_t corresponding to flume bed.

[b] u_{*b} is shear velocity from slope-depth relationship corrected for sidewall effect according to Nezu and Nakagawa (1993, pp. 94, 95).

[c] u_{*L} is shear velocity from logarithmic formula (22) assuming $\kappa = 0.40$.

[d] $u_* = (u_{*s} + u_{*L} + u_{*b})/3$.

J. Hydraul. Eng. 2001.127:123-133.

Flow Type 2 ($(2-5)\Delta > H \geq \Delta \sim \delta$)

We can reasonably postulate that the linear relationship (23) is valid over the whole depth for this flow type, with the same δ and C as for the flow type 1. This is because there is no overlap region and the flow above the roughness elements is heavily influenced by eddies of scale δ generated in the wakes of roughness elements. These eddies strongly dominate over eddies which scale with Z. The depth-averaged velocity $\langle\overline{u}\rangle_a$ for this flow type may be defined as either $\langle\overline{u}\rangle_a = (1/H)\int_0^H \langle\overline{u}\rangle(Z)\,dZ$ or $\langle\overline{u}\rangle_a = (1/H_a)\int_0^H \langle\overline{u}\rangle(Z)A(Z)\,dZ$, where $H_a = \int_0^{Z_{ws}} A(Z)\,dZ$ and $A = A_f/A_0$ is nondimensional area. The second definition is more appropriate as it satisfies the mass conservation condition, i.e., the specific flow rate $q = \langle u\rangle_a H_a$. Following this second definition for $\langle\overline{u}\rangle_a$, we can obtain using (23)

$$\sqrt{\frac{8}{f}} = \frac{\langle\overline{u}\rangle_a}{u_*} = Cm\,\frac{H}{\delta} \quad \text{or} \quad f = \frac{8u_*^2}{\langle\overline{u}\rangle_a^2} = \frac{8}{C^2m^2}\left[\frac{\delta}{H}\right]^2 \tag{24}$$

where f = Darcy-Weisbach friction factor; $H = z_{ws} - z_t$ = maximum depth; and $m = (1/H_aH)\int_0^H ZA(Z)\,dZ$ = parameter that depends on the roughness geometry function $A(Z)$. For $A(Z)$ from Fig. 3 the parameter m is weakly dependent on H, and, as a first approximation, may be considered as a constant, $m \approx 0.6$. To test relationship (24) we use the hydraulic resistance data for shallow gravel-bed flows reported by Bathurst et al. (1981). Their experiments were conducted in a flume with a bed covered by one layer of gravel particles. Fig. 5 shows Bathurst et al.'s (1981) data as well as a curve presenting relationship (24) with $M = (8/C^2m^2) = 1.2$. The thickness δ in Fig. 5 is defined as the appropriate maximum size of the short particle axis. One can see from Fig. 5 that relationship (24) agrees with Bathurst et al.'s (1981) data fairly well, at least in the range of δ/H from approximately 0.4 to 1.25, which is equivalent to the range of H/δ from approximately 0.8 to 2.5. The parameter $M = (8/C^2m^2)$ for this data set ranges from 0.4 to 2.5. For comparison, we have also plotted in Fig. 5 field data reported in Bathurst (1985b), assuming that $\delta/H \approx D_{84}/H_{\text{mean}}$, where H_{mean} is the cross section mean depth. An additional support for relationships (24) may be found in Day (1978) and Bathurst (1994) who reported laboratory and field data covering the range $0.6 \leq H/D_{90} \leq 5$. In most cases their graphs $U/u_* = F(H/D_{84})$ and $U/u_* = F(H/D_{90})$ may be approximated as $\langle\overline{u}\rangle_a/u_* \sim U/u_* = K[H/D_{84\,\text{or}\,90}]$ with K in the range from 1.8 to 4.0. Assuming that $\delta \approx D_{84} \approx D_{90}$, $m \approx 0.6$, and using (24) we can estimate the range of C from 3 to 7.

Flow Type 3 ($H < \Delta \sim \delta$)

The thickness of δ_I of the interfacial sublayer as well as relationship (23) become irrelevant for this flow type. However, relationship (20) is still applicable, though it requires a new formulation for ν_I. We accept in our consideration a simple relationship $\nu_I = (1/\alpha)H_a u_*$, where α is a coefficient (similar to C) which depends on bed geometry. Assuming that $\tau(Z)/\rho \approx \tau_0/\rho = u_*^2$, $\langle\overline{u}\rangle = 0$ at $Z = 0$, and also, that α does not change with Z, we can obtain from (20)

$$\frac{\langle\overline{u}\rangle}{u_*} = \frac{u_*}{\nu_I}Z = \alpha\,\frac{Z}{H_a} \tag{25}$$

Comparing (23) and (25) one can obtain a relationship between C and α as $C = \alpha(\delta/H_a)$. The hydraulic resistance relationships follow from relationship (25) as

$$\sqrt{\frac{8}{f}} = \frac{\langle\overline{u}\rangle_a}{u_*} = \alpha m\,\frac{H}{H_a} \quad \text{or} \quad f = \frac{8u_*^2}{\langle\overline{u}\rangle_a^2} = \frac{8}{\alpha^2m^2}\left[\frac{H_a}{H}\right]^2 \tag{26}$$

where m has a similar meaning as in relationship (24). Unfortunately, the appropriate data sets that could be used to test relationships (25) and (26) are not available. However, some speculations based on (26) are possible. As an example, for a range of rough surfaces the function $H_a = F(H)$ grows faster than $H_a \propto H$ that gives an increase in f with increase in H. If we further assume that $H_a \approx \gamma H^2/\Delta$ where $\Delta \approx \delta_I = \delta$ and $\gamma \approx 0.6$, which are suggested by Bathurst et al.'s (1981) data, relationships (26) may be rewritten as

$$\sqrt{\frac{8}{f}} = \frac{\langle\overline{u}\rangle_a}{u_*} = \frac{\alpha m}{\gamma}\,\frac{\delta}{H} \quad \text{or} \quad f = \frac{8u_*^2}{\langle\overline{u}\rangle_a^2} = \frac{8\gamma^2}{\alpha^2m^2}\left[\frac{H}{\delta}\right]^2 \tag{27}$$

Comparing (24) and (27) one can obtain relationships between C, α, and γ as $C = \alpha(\delta/H_a) = \alpha/\gamma$ and $\gamma = H_a/\delta$. Relationships (27) have the same arguments as those for flow types 1 and 2. This makes it possible to combine all three relationships for $f = F(H/\delta)$ for a wide range of H/δ as shown in Fig. 6. A noticeable property of $f = F(H/\delta)$ in Fig. 6 is a maximum at $H/\delta \approx 1$ whose approximate value can be evaluated from (24) as $8/C^2m^2$. There is also a transition region between flow types 1 and 2. This region is a result of superposition of wake eddies, separated from roughness elements, and eddies generated due to velocity shear and scaled with Z. The function $f = F(H/\delta)$ in Fig. 6 is supported by data for overland flows compiled by Lawrence (1997) from different sources and presented as plots of $f = F(H/\Delta)$ for the range $0.01 < H/\Delta < 300$. Lawrence (1997) also provided some support for such a behavior of $f = F(H/\Delta)$ though, unfortunately, her considerations were based on time-averaged velocities as in Nikitin's (1963) study.

The bed permeability should modify the above considerations as the nonslip condition becomes invalid. However, it is believed that the structure of the relationships suggested for impermeable beds should still apply.

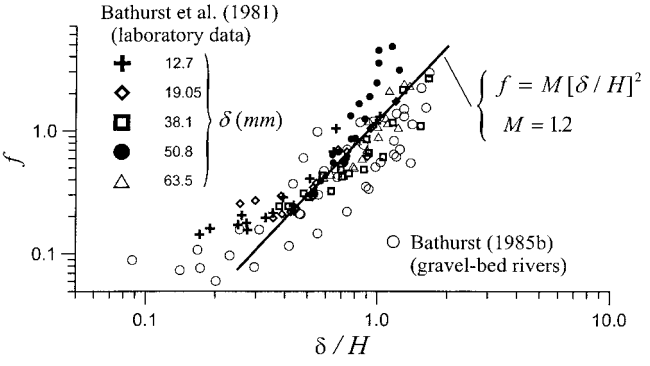

FIG. 5. Comparison of Eq. (24) with Laboratory Data of Bathurst et al. (1981) and with Field Data of Bathurst (1985b)

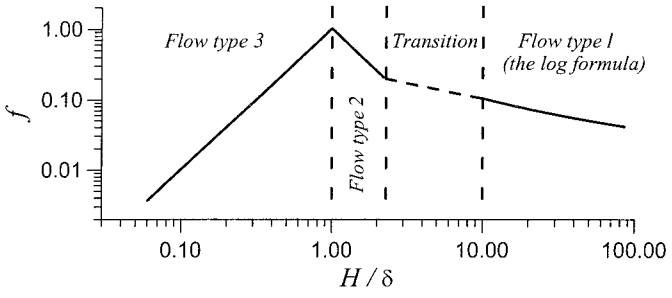

FIG. 6. Sketch Showing Friction Factor As Function of Relative Submergence, As Follows from Eqs. (24)–(27); Note that Peak Value of f and Boundaries of Transition Region May Depend on Roughness Geometry

J. Hydraul. Eng. 2001.127:123-133.

TURBULENCE CHARACTERISTICS

The methodology based on the spatially averaged flow variables should be also used in characterizing turbulence properties near rough beds. Conventional time-averaged velocity moments $\overline{u_i'^{\alpha}u_j'^{\beta}u_k'^{\gamma}}$ (e.g., the turbulence intensity or Reynolds stresses) will be strongly influenced by local conditions within the roughness layer, and therefore, cannot be representative. Instead, double-averaged moments, $\langle\overline{u_i'^{\alpha}u_j'^{\beta}u_k'^{\gamma}}\rangle$, should be used, as suggested by (4)–(7). Also, for a more complete flow description these double-averaged turbulence moments should be supplemented with form-induced moments $\langle\tilde{u}_i^{\alpha}\tilde{u}_j^{\beta}\tilde{u}_k^{\gamma}\rangle$, which characterize disturbances in the time-averaged flow. To illustrate this approach we use our ADV measurements in the spherical segment-bed flume described above (Table 1; Fig. 4). These measurements provide estimates for some of the velocity moments, i.e., $\langle\overline{u'^2}\rangle$, $\langle\overline{v'^2}\rangle$, $\langle\overline{w'^2}\rangle$, $\langle\overline{u'w'}\rangle$, $\langle\tilde{u}^2\rangle$, $\langle\tilde{v}^2\rangle$, $\langle\tilde{w}^2\rangle$, and $\langle\tilde{u}\tilde{w}\rangle$. Fig. 7 shows the vertical distribution of the normalized time-averaged turbulence intensities $\overline{u'^2}/u_*^2$, $\overline{v'^2}/u_*^2$, $\overline{w'^2}/u_*^2$, and the Reynolds stress $-\overline{u'w'}/u_*^2$ at several neighboring horizontal locations shown in Fig. 4(a), as well as polynomial fits to these data (solid curves) which represent the corresponding double-averaged parameters $\langle\overline{u'^2}\rangle/u_*^2$, $\langle\overline{v'^2}\rangle/u_*^2$, $\langle\overline{w'^2}\rangle/u_*^2$, and $-\langle\overline{u'w'}\rangle/u_*^2$. The deviations of the normalized time-averaged values from their double-averaged counterparts in Fig. 7 reduce with increase in Z, being the largest, up to 50–100%, in the range $Z/\delta < 2.0$. These deviations may be interpreted as form-induced fluctuations due to the influence of local conditions. To evaluate the form-induced intensities $\langle\tilde{u}^2\rangle/u_*^2$, $\langle\tilde{v}^2\rangle/u_*^2$, and $\langle\tilde{w}^2\rangle/u_*^2$, and the form-induced stress $-\langle\tilde{u}\tilde{w}\rangle/u_*^2$ we use the same procedure as in Fig. 7, i.e., the polynomial fitting of point values $\tilde{u}^2/u_*^2$, $\tilde{v}^2/u_*^2$, $\tilde{w}^2/u_*^2$, and

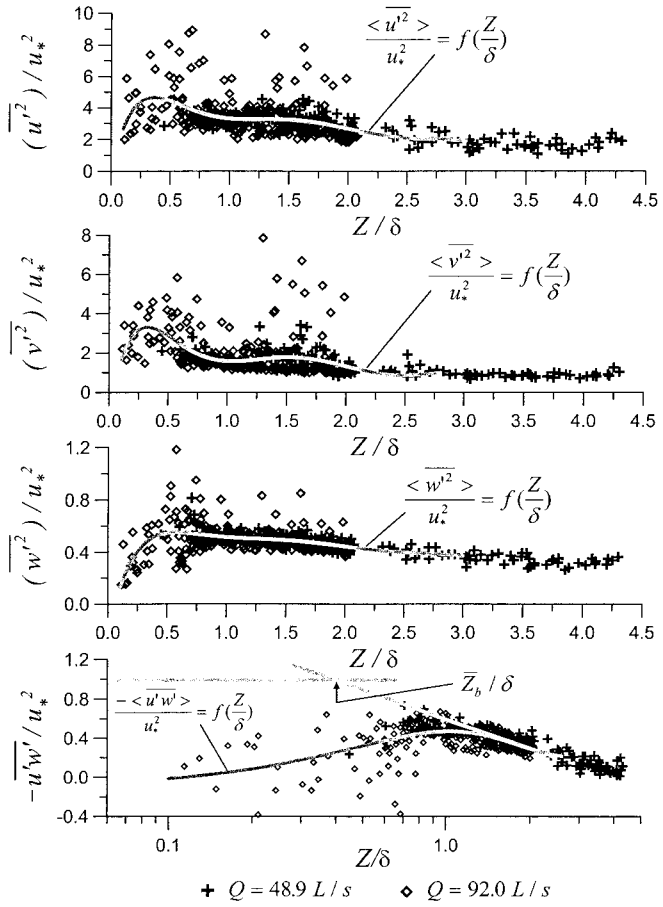

FIG. 7. Vertical Distribution of Relative Turbulence Intensities and Reynolds Stress (for Spherical Segment-Type Bed Roughness Shown in Fig. 4); Solid Lines Are Polynomial Fit

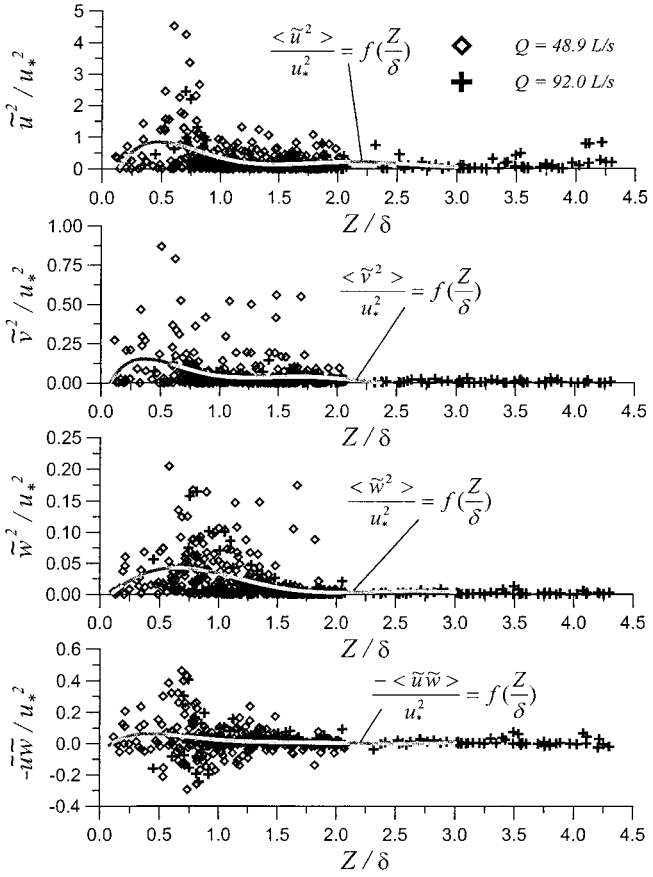

FIG. 8. Vertical Distribution of Relative Form-Induced Intensities and Form-Induced Stress (for Spherical Segment-Type Bed Roughness Shown in Fig. 4); Solid Lines Are Polynomial Fit

$-\tilde{u}\tilde{w}/u_*^2$ (Fig. 8). As one would expect, the form-induced intensities attain maximum values within the interfacial sublayer ($Z/\delta < 1.0$), then reduce with increase in Z, and become negligible at $Z/\delta > 2.0$. All form-induced intensities are significantly smaller than their turbulent counterparts. The form-induced stress $-\langle\tilde{u}\tilde{w}\rangle/u_*^2$ is negligible within the form-induced sublayer, and becomes comparable (though less) with $-\langle\overline{u'w'}\rangle/u_*^2$ in the interfacial sublayer (Fig. 8). The above estimates of double-averaged intensities and stresses characterize the near-bed flow structure for the regular spherical segment-type roughness and may not be applicable for nonuniform gravel beds.

CONCLUSIONS

In this paper we suggest that the double-averaged (in temporal and in spatial domains) momentum equations should be used as a natural basis for hydraulics of rough-bed open-channel flows, especially with small relative submergence. The main advantages of this approach include: (1) a consistent link between spatially averaged roughness parameters and double-averaged flow variables; (2) the appearance of a form drag term and form-induced stresses in the momentum equations as a result of rigorous derivation rather than intuitive reasoning; (3) the possibility for scaling considerations and parameterizations based on double-averaged variables which may cover all flow regions including the interfacial sublayer; and (4) the possibility for the consistent scale partitioning of the roughness parameters and flow properties, for the case of multiscale roughnesses (e.g., grain and bed-form roughnesses). The difference between the double-averaged equations and the time-averaged Reynolds equations is as fundamental as that between Reynolds equations and Navier-Stokes equations for

J. Hydraul. Eng. 2001.127:123-133.

instantaneous velocities and pressure. The results of our analysis of the double-averaged momentum equations and scaling and phenomenological considerations of the double-averaged variables may be summarized as follows:

1. Five specific flow regions with qualitatively different properties are suggested, subject to $H >> \Delta$: (1) the outer layer; (2) the logarithmic layer; (3) the form-induced sublayer; (4) the interfacial sublayer (the sum of the latter two is the roughness layer); and, for the case of permeable beds, (5) the subsurface layer.
2. Three flow types may be distinguished from the above flow subdivision: (1) flow with high relative submergence ($H >> \Delta$), which contains all the above flow regions; (2) flow with small relative submergence [$(2 - 5)\Delta > H \geq \Delta$], with the form-induced sublayer as the upper flow region; and (3) flow over a partially inundated rough bed ($H < \Delta$), with the interfacial sublayer as the upper flow region.
3. The relationships for the vertical distribution of the total stress for the simplest case of 2D, steady, uniform, spatially-averaged flow over a rough bed with flat free surface are derived. These relationships explicitly include the form-induced stresses and form drag as components of the total stress.
4. The relationships for the double-averaged velocity distribution and hydraulic resistance for the flow types 1, 2, and 3 have been derived and compared with the measurements where possible. These relationships, though promising, should be considered as preliminary approximations that need additional tests.
5. The double-averaged turbulence and form-induced intensities and stresses have been evaluated for the case of regular spherical segment-type roughness. They show the dominant role of the double-averaged turbulence stresses and the form drag in the momentum transfer in the near-bed region.
6. Most existing data sets of rough-bed flows are based on point measurements for a selected vertical, and therefore, are not sufficient to characterize double-averaged flow properties. We believe that new experimental studies of rough-bed flows should be designed to get double-averaged flow variables. Newly developed measurement technologies (e.g., particle image velocimetry, etc.) make such a task realistic.

In this paper we have considered the simplest case of 2D, steady, uniform, spatially averaged flow over a rough bed with flat free surface. In further studies our analysis could be extended to cover the more realistic case of nonuniform rough-bed flows with nonflat water surface. For this case, a water surface geometry function $A_{ws}(Z)$, analogous to the roughness geometry function $A(Z)$, should be taken into consideration. Another issue that still requires attention is definition for the reference bed and the thickness of the interfacial sublayer δ. The definition of these parameters may depend on bed roughness geometry and should be developed on a wider experimental data base involving different roughness types.

ACKNOWLEDGMENTS

This research was conducted under Contracts CO1818 (analysis) and CO1813 (measurements) from the Foundation for Research, Science, and Technology (New Zealand). Ian McEwan was supported by the National Institute of Water and Atmospheric Research, New Zealand, and the Royal Academy of Engineering of the U.K. The measurements were made by S. Brown and R. Smith. Discussions with S. McLean, G. Parker, A. Dittrich, and M. Garcia are greatly appreciated. Three anonymous reviewers provided thorough reviews and helpful suggestions.

APPENDIX I. REFERENCES

Bathurst, J. C. (1985a). ''Theoretical aspects of flow resistance.'' *Gravel-bed rivers*, R. D. Hey, J. C. Bathurst, and C. R. Thorne, eds., Wiley, New York, 83–108.
Bathurst, J. C. (1985b). ''Flow resistance estimation in mountain rivers.'' *J. Hydr. Engrg.*, ASCE, 111(4), 625–643.
Bathurst, J. C. (1994). ''At-a-site mountain river flow resistance variation.'' *Proc., Hydr. Engrg. '94*, ASCE, New York, 682–686.
Bathurst, J. C., Simmons, D. B., and Li, R.-M. (1981). ''Resistance equation for large-scale roughness.'' *J. Hydr. Div.*, ASCE, 107(12), 1593–1613.
Bray, D. I. (1985). ''Flow resistance in gravel-bed rivers.'' *Gravel-bed rivers*, R. D. Hey, J. C. Bathurst, and C. R. Thorne, eds., Wiley, New York, 109–132.
Day, T. J. (1978). ''Aspects of flow resistance in steep channels having coarse particulate beds.'' *Research in fluvial geomorphology*, R. Davidson-Arnott and W. Nickling, eds., University of Guelph, Ont., 45–58.
Dittrich, A., and Koll, K. (1997). ''Velocity field and resistance of flow over rough surface with large and small relative submergence.'' *Int. J. Sediment Res.*, 12(3), 21–33.
Finnigan, J. J. (1985). ''Turbulent transport in flexible plant canopies.'' *The forest-atmosphere interactions*, B. A. Hutchinson and B. B. Hicks, eds., Reidel, Dordrecht, The Netherlands, 443–480.
Gimenez-Curto, L. A., and Corniero Lera, M. A. (1996). ''Oscillating turbulent flow over very rough surfaces.'' *J. Geophys. Res.*, 101(C9), 20745–20758.
Graf, W. H., and Altinakar, M. S. (1998). *Fluvial hydraulics*, Wiley, New York.
Griffiths, G. A. (1981). ''Flow resistance in coarse gravel bed rivers.'' *J. Hydr. Div.*, ASCE, 107(7), 899–918.
Grinvald, D. I., and Nikora, V. I. (1988). *River turbulence*, Hydrometeoizdat, Leningrad, Russia (in Russian).
Izakson, A. (1937). ''Formula for the velocity distribution near a wall.'' *J. Experimental and Theoretical Phys. (Zh. Eksp. Teor. Fiz.)*, 7, 919–924 (in Russian).
Kironoto, B. A., and Graf, W. H. (1994). ''Turbulence characteristics in rough uniform open-channel flow.'' *Proc., Instn. Civ. Engrg. Water, Maritime, and Energy*, 106, 333–344.
Kraus, N. C., Lohrmann, A., and Cabrera, R. (1994). ''New acoustic meter for measuring 3D laboratory flows.'' *J. Hydr. Engrg.*, ASCE, 120(3), 406–412.
Lawrence, D. S. L. (1997). ''Macroscale surface roughness and frictional resistance in overland flow.'' *Earth Surface Processes and Landforms*, 22, 365–382.
Lindsey, R. K., Kohler, M. A., and Paulhus, J. L. H. (1975). *Hydrology for engineers*, McGraw-Hill, New York.
Lohrmann, A., Cabrera, R., and Kraus, N. C. (1994). ''Acoustic-Doppler velocimeter (ADV) for laboratory use.'' *Proc., Symp. on Fundamentals and Advancements in Hydr. Measurements and Experimentation*, C. A. Pugh, ed., ASCE, New York, 351–365.
Lopez, F., and Garcia, M. (1996). ''Turbulence structure in cobble-bed open-channel flow.'' *Hydr. Engrg. Ser. No. 52*, University of Illinois at Urbana-Champaign, Ill., 139.
Millikan, C. B. (1939). ''A critical discussion of turbulent flows in channels and circula tubes.'' *Proc., 5th Int. Congr. Appl. Mech.*, 386–392.
Monin, A. S., and Yaglom, A. M. (1971). *Statistical fluid mechanics: Mechanics of turbulence*, Vol. 1, MIT Press, Cambridge, Mass.
Nezu, I., and Nakagawa, H. (1993). *Turbulence in open-channel flows*, Balkema, Rotterdam, The Netherlands.
Nikitin, I. K. (1963). *Turbulent channel flow and processes in the near-bed region*, Ukraine Acad. Sci., Kiev, Ukraine (in Russian).
Nikitin, I. K. (1980). *Complex turbulent flows and heat and mass transfer processes*, Ukraine Acad. Sci., Kiev, Ukraine (in Russian).
Nikora, V. I., and Goring, D. G. (1998). ''ADV measurements of turbulence: Can we improve their interpretation?'' *J. Hydr. Engrg.*, ASCE, 124(6), 630–634.
Nikora, V. I., Goring, D. G., and Biggs, B. J. F. (1998a). ''On gravel-bed roughness characterisation.'' *Water Resour. Res.*, 34(3), 517–527.
Nikora, V. I., Goring, D. G., and Biggs, B. J. F. (1998b). ''Silverstream eco-hydraulics flume: Hydraulic design and tests.'' *NZ J. of Marine and Freshwater Res.*, 32, 607–620.
Nikora, V. I., and Smart, G. M. (1997). ''Turbulence characteristics of New Zealand gravel-bed rivers.'' *J. Hydr. Engrg.*, ASCE, 123(9), 764–773.
Raupach, M. R., Antonia, R. A., and Rajagopalan, S. (1991). ''Rough-wall turbulent boundary layers.'' *Appl. Mech. Rev.*, 44(1), 1–25.
Raupach, M. R., and Shaw, R. H. (1982). ''Averaging procedures for flow within vegetation canopies.'' *Boundary-Layer Meteorology*, 22, 79–90.

J. Hydraul. Eng. 2001.127:123-133.

Shimizu, Y., Tsujimoto, T., and Nakagawa, H. (1990). "Experiment and macroscopic modelling of flow in highly permeable porous medium under free-surface flow." *J. Hydrosci. and Hydr. Engrg.*, 8(1), 69–78.
Smith, J. D., and McLean, S. R. (1977). "Spatially averaged flow over a wavy surface." *J. Geophys. Res.*, 83(12), 1735–1746.
Song, T., and Graf, W. H. (1994). "Nonuniform open-channel flow over a rough bed." *J. Hydrosci. and Hydr. Engrg.*, 12(1), 1–25.
Townsend, A. A. (1998). *The structure of turbulent shear flows*, Cambridge University Press, London.
Wilson, N. R., and Shaw, R. H. (1977). "A higher order closure model for canopy flow." *J. Appl. Meteorology*, 16, 1197–1205.

APPENDIX II. NOTATION

The following symbols are used in this paper:

A = ratio of area A_f occupied by fluid within fixed region on x,y-plane to total area A_0 of region;
A_f = area occupied by fluid within fixed region on x,y-plane with total area A_0;
C = parameter of velocity distribution, $C = \langle\overline{u}\rangle(\delta)/u_*$;
D = particle size;
f = Darcy-Weisbach friction factor;
H = maximum flow depth equal to distance between water surface and troughs of roughness elements, i.e., $H = z_{ws} - z_t$ (Fig. 2);
H_a = mean depth;
M = $(8/C^2m^2)$;
m = parameter depending on roughness geometry;
S_b = bed slope;
U = depth-averaged flow velocity for flow type 1;
u, v, w = instantaneous longitudinal, transverse, and vertical velocity components, respectively;
$\overline{u}, \overline{v}, \overline{w}$ = time-averaged longitudinal, transverse, and vertical velocity components, respectively;
$\langle\overline{u}\rangle, \langle\overline{v}\rangle, \langle\overline{w}\rangle$ = double-averaged (in time and spatial domains) velocities;
$\tilde{u}, \tilde{v}, \tilde{w}$ = form-induced velocity components, i.e., $\tilde{u}_i = \overline{u}_i - \langle\overline{u}_i\rangle$;
$\langle\overline{u}\rangle_d$ = depth-averaged velocity for flow types 2 and 3;
$\overline{u_i'u_j'}$ = time-averaged Reynolds (turbulent) stress;
$\langle\overline{u_i'u_j'}\rangle$ = double-averaged Reynolds (turbulent) stress;
$\langle\tilde{u}_i\tilde{u}_j\rangle$ = form-induced stress;
u_* = shear velocity, i.e., $u_* = (\tau_0/\rho)^{0.5}$;
$\langle\overline{\tilde{u}_i^{\alpha}\tilde{u}_j^{\beta}\tilde{u}_k^{\gamma}}\rangle$ = form-induced velocity moments;
$\overline{u_i'^{\alpha}u_j'^{\beta}u_k'^{\gamma}}$ = time-averaged velocity moments;
$\langle\overline{\tilde{u}_i'^{\alpha}\tilde{u}_j'^{\beta}\tilde{u}_k'^{\gamma}}\rangle$ = double-averaged velocity moments;
x, y, z = coordinate axes oriented along main flow parallel to averaged bed, to left bank, and toward water surface, respectively;
Z_b = bed elevation;
$\overline{Z}_b$ = mean bed elevation;
z_c = elevation of highest roughness crests;
z_f = elevation of impermeable floor supporting particles;
z_L = elevation of upper bound of logarithmic layer;
z_R = elevation of lower bound of logarithmic layer or upper bound of roughness layer;
z_t = elevation roughness troughs where $A = 0$ (impermeable bed) or $dA/dz = 0$ (permeable bed);
z_{ws} = elevation of water surface;
Δ = roughness height;
δ = boundary between logarithmic and linear flow regions when coordinate $Z = z - z_t$ is used;
δ_F = thickness of form-induced sublayer, $\delta_F = z_R - z_c$;
δ_I = thickness of interfacial sublayer, $\delta_I = z_c - z_t$;
δ_R = thickness of roughness layer $\delta_R = z_R - z_t$;
κ = von Kármán constant; and
τ_0 = bed shear stress.

J. Hydraul. Eng. 2001.127:123-133.